Journal of the Brazilian Society of Mechanical Sciences and Engineering (2019) 41:300
https://doi.org/10.1007/s40430-019-1805-9

TECHNICAL PAPER

# Multi-objective optimization of some correlated process parameters in EDM of Inconel 800 using a hybrid approach

T. R. Paul[1] · A. Saha[2] · H. Majumder[1] · V. Dey[1] · P. Dutta[1]

Received: 26 December 2018 / Accepted: 24 June 2019 / Published online: 29 June 2019


## Abstract
Electrical discharge machining (EDM) is an extensively used non-traditional machining process used for conductive materials to get intricate or complex shapes. For any manufacturing industry, optimum parameters of control variables are of sheer importance to improve multiple performance characteristics like surface integrity and productivity. This paper presents multi-objective optimization on the basis of ratio analysis (MOORA) method coupled with principal component analysis (PCA) in order to achieve the optimal combination of EDM parameters. In this research work, response surface methodology was used for designing the experiments considering three input parameters, namely pulse-on time, pulse-off time and pulsed current. All the experiments were conducted at different parametric combinations and the performance, namely material removal rate (MRR) and surface roughness ($R_a$). Proposed MOORA-PCA hybrid results and conventional MOORA results were compared, and it is found that proposed methods are accurate for predicting the responses. Finally, the control variables, namely pulse-on time ($T_{ON}$), pulse-off time ($T_{OFF}$) and pulsed current ($I_p$), were set to 300 µs, 85 µs and 18 A, respectively, to get maximum MRR and minimum surface roughness.

**Keywords** Multi-objective optimization · Inconel 800 · MOORA · PCA · Surface roughness

## 1 Introduction

Electrical discharge machining (EDM) is a non-contact, highly stochastic and complex, most widely used non-traditional machining method where thermo-electrical energy is used to erode material from the workpiece [1, 2]. In this process, with the help of pulse generator, a succession of discrete sparks is generated between the minute gap of workpiece and electrode. A dielectric fluid, which is flushed through this narrow gap, removes the tiny parts of the workpiece. EDM, which has high accuracy, is extensively used to machine difficult-to-cut conductive materials. This process is readily used to machine intricate three-dimensional complex shapes and, thus, is massively used in tool, moulds and die-making industry [3].

With the advancement of human lifestyle, it has become necessary to improve existing materials and the processes to manufacture using such materials. One such material is superalloy. This is widely used in equipment for chemical and petrochemical industry, heat treatment process, nuclear power plant. A superalloy is very difficult to machine by conventional machining techniques. The surface finish of the machined surface is poor with high tool wear [4]. In this situation, EDM is found to be a well-suited non-traditional machining process, which can be adapted to machine this kind of difficult-to-cut materials.

There is a competition, among the manufacturers to minimize manufacturing price. In any machining operation, this is generally done by increasing material removal rate (MRR). This, however, brings a toll on the quality of the machined surface. The conflicting nature of the outputs makes it difficult to pick the best ideal setting. Thus, the presence of the contrary responses makes it more mindboggling to select the best input parameter setting. To overcome such problem, people, nowadays, use modern optimization techniques to generate a mathematical model to visualize the outcomes, by suggesting

Technical Editor: Lincoln Cardoso Brandao.

✉ H. Majumder
himu.nita@gmail.com

1 Production Engineering Department, National Institute of Technology, Agartala, Agartala 799046, India

2 Production Engineering Department, Haldia Institute of Technology, Haldia, West Bengal 721657, India

appropriate inputs, before implementing them in actual production. There are different multi-objective optimization techniques available to help this selection process. Among them, multi-objective optimization on the basis of ratio analysis (MOORA) is seen to be very simple and mathematically easy to use [5]. In real-life problem, as the percentage contribution of each response is not equal, there is a need to find the relative impact of the responses. Principal component analysis (PCA), a statistical method, is adopted to find the weight percentage of each response.

Ho et al. [6] reviewed different research works executed in the development of die-sinking EDM in the past decades for the enhancement of the machining characteristics. Khan et al. [7] successfully used MOORA method for different non-traditional processes and concluded that this is a precise process that is easy in operation and saves time. Chakravorty et al. [8] used PCA-based different optimizations to optimize past experimental data and showed the capability of PCA to optimize multiple responses in EDM. Bhaumik et al. [9] utilized a hybrid optimization technique in EDM where desirability was coupled with grey relational analysis (GRA), to ascertain optimum setting of the input parameters for higher MRR and lower tool wear rate (TWR). Besides the use of MOORA technique in non-traditional machines, it has been effectively executed for the parametric optimization of numerous other manufacturing processes like milling [10], turning [11], welding [12], etc. PCA was also successfully utilized, coupled with other multi-objective optimization approaches, to identify optimal process parameters in welding [13–16], turning [17, 18], WEDM [19, 20], etc.

Decision makers face a lot of problems with multiple and conflicting criteria. Multiple attribute decision-making (MADM) helps the decision makers for making preference decisions over available alternatives. There are several common methodologies for MADM, such as the technique for order preference by similarity to ideal solution (TOPSIS), desirability function analysis (DFA), multi-objective optimization on the basis of ratio analysis (MOORA). From the review of past literature, it is quite clear that several experimental works have been made on EDM/WEDM of different grades of materials such as nanostructured hardfacing alloy and metal matrix composites[21–24]. However, very few experimental works are reported on multi-objective optimization of Inconel 800. It is well known that the Inconel 800 is a kind of a difficult-to-cut material. Therefore, at this stage, extensive research is needed to check the best machining condition in EDM of Inconel 800.

So, this study explores to apply MOORA, coupled with PCA, while machining Inconel 800 (iron–nickel–chromium alloy) using EDM. Our analysis is focused on changing three key input parameters such as pulse-on time ($T_{ON}$), pulse-off time ($T_{OFF}$) and pulsed current ($I_P$) on the MRR and surface roughness ($R_a$) to build up the optimization model.

## 2 Materials and method

This part of the manuscript explains EDM machining of Inconel 800 to collect experimental data and then explains how PCA-MOORA model optimizes the input parameters.

### 2.1 Experimental setup

During this study, the experiment of EDM machining on Inconel 800 was conducted on a die-sinking EDM. The effect of the variation in input parameters, pulse-on time ($T_{ON}$), pulse-off time ($T_{OFF}$) and pulsed current ($I_P$) on the MRR and surface roughness ($R_a$), was studied. Based on available literature, practical experience and trial and error method, the input parameter was selected [25–29].

### 2.2 Machine tool

The entire work has been carried out on a die-sinking EDM machine with model SPARKONIX MOS 25A. The dielectric was flushed at a pressure of 0.2 kgf/cm$^2$. The copper electrode was kept positive during the experiment. A pulsed discharge current in positive mode was applied in steps.

### 2.3 Workpiece material

The most important feature to take into concern is the right selection of the workpiece material in an EDM process. The workpiece material used in this study was Inconel 800 (25 mm × 25 mm × 5 mm). This austenitic, solid-solution alloy has a high tensile strength at high temperature and high impact strength at room temperature. The chemical composition of the workpiece is shown in Table 1. The presence of chromium makes it corrosion and oxidation resistant, nickel makes the material resistant towards scaling and stress-corrosion cracking, and finally, silicon helps Inconel to become heat resistant.

**Table 1** Chemical composition of Inconel 800

| | Ni | Cr | Co | Silicon | C | Al | Ti | Copper | Mn | Sulphur | Iron |
|---|---|---|---|---|---|---|---|---|---|---|---|
| Minimum | 30 | 19 | – | | – | 0.15 | 0.15 | – | – | – | Balance |
| Maximum | 35 | 23 | 2 | 1.00 | 1.00 | 0.60 | 0.60 | 0.75 | 1.50 | 0.015 | |

### 2.4 Electrode material

In this research, the electrode was made up of oxygen free high conductivity copper (OFHC). OFHC type of electrode used mainly because it is made of pure copper and the percentage of copper is 99.99%.

### 2.5 Experimental procedure

Experiments on Inconel 800 were conducted based on the design of experiment called response surface methodology (RSM). A total of 51 experiments were carried out at different levels of the parameters. The responses are surface roughness ($R_a$) and material removal rate (MRR). The weight of the specimens was measured on a CPA 225D Sartorious electronic balance. By calculating the difference, in the weights, before and after machining the material removal was calculated. Machining time was kept fixed at 25 min for all experiment. Consequently, the MRR was calculated by dividing the weight difference by the time of machining (25 min) for all the cases to get the machining rate per unit time. After measuring the weight, the surface finish of the die sunk specimen has been analysed under Taylor Hobson 3D surface profilometer. The scan-off length and cut-off length was found to be 0.86 mm and 3.59 mm, respectively, for all the investigations. Surface roughness in the form of Ra was calculated as an average of 20 points spread across the machined surface. The experimental layout is shown in Fig. 1.

### 2.6 Methodology

In this study, a multi-objective optimization technique combining with multi-objective optimization on the basis of ratio analysis (MOORA) method and principal component analysis (PCA) has been used to optimize different responses.

#### 2.6.1 Multi-objective optimization on the basis of ratio analysis (MOORA)

MOORA, a robust decision-making approach, was first presented by Brauers [30, 31]. Various steps that are followed in MOORA are:

*Step 1:* Identify the problem

The first step is to delineate the objective and recognize all appropriate alternatives and their qualities.

*Step 2:* Establish a decision matrix

After recognizing the objectives and alternatives, the next step for MOORA is to establish the decision matrix alike any multi-objective optimization techniques.

$$A = \begin{bmatrix} a_{11} & a_{12} & \dots & \dots & a_{1n} \\ a_{21} & a_{22} & \dots & \dots & a_{2n} \\ \dots & \dots & \dots & \dots & \dots \\ \dots & \dots & \dots & \dots & \dots \\ a_{m1} & a_{m2} & \dots & \dots & a_{mm} \end{bmatrix} \quad (1)$$

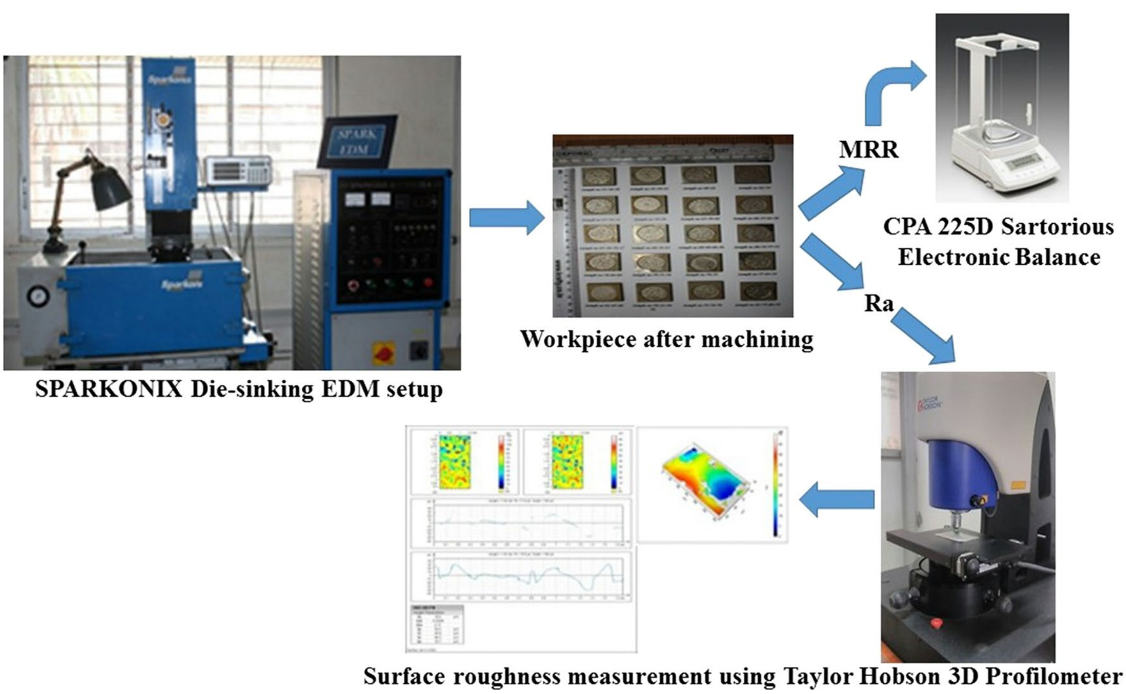


**Fig. 1** Experimental layout

**Table 2** Design matrix and experimental results

| Exp. no. | $T_{ON}$ (μs) | $T_{OFF}$ (μs) | $I_p$ (Amp.) | Weight before EDM [$W_s$] (g) | Weight after EDM [$W_f$] (g) | Difference $W_d = W_s - W_f$ | MRR [$W_d$/25] (gm/min) | Average surface roughness [$R_a$] (μm) |
|---|---|---|---|---|---|---|---|---|
| 1 | 100 | 20 | 12 | 25.0193 | 23.3393 | 1.680 | 0.067 | 3.835 |
| 2 | 500 | 20 | 12 | 24.9113 | 21.0363 | 3.875 | 0.155 | 3.175 |
| 3 | 100 | 150 | 12 | 25.6776 | 25.1512 | 0.526 | 0.021 | 3.320 |
| 4 | 500 | 150 | 12 | 24.8828 | 22.1828 | 2.700 | 0.108 | 3.593 |
| 5 | 100 | 20 | 18 | 25.3344 | 22.7088 | 2.626 | 0.105 | 3.665 |
| 6 | 500 | 20 | 18 | 25.2525 | 18.1275 | 7.125 | 0.285 | 3.400 |
| 7 | 100 | 150 | 18 | 25.9126 | 25.3269 | 0.586 | 0.023 | 3.937 |
| 8 | 500 | 150 | 18 | 24.6705 | 19.7955 | 4.875 | 0.195 | 4.385 |
| 9 | 100 | 85 | 15 | 24.7140 | 23.614 | 1.100 | 0.044 | 3.478 |
| 10 | 500 | 85 | 15 | 24.7384 | 20.1384 | 4.600 | 0.184 | 3.295 |
| 11 | 300 | 20 | 15 | 22.9886 | 19.9386 | 3.050 | 0.122 | 4.267 |
| 12 | 300 | 150 | 15 | 24.8459 | 22.8959 | 1.950 | 0.078 | 4.200 |
| 13 | 300 | 85 | 12 | 24.8667 | 22.3667 | 2.500 | 0.100 | 4.149 |
| 14 | 300 | 85 | 18 | 24.8158 | 20.4658 | 4.350 | 0.174 | 4.725 |
| 15 | 300 | 85 | 15 | 22.9695 | 20.1695 | 2.800 | 0.112 | 4.178 |
| 16 | 300 | 85 | 15 | 23.5157 | 20.7157 | 2.800 | 0.116 | 4.052 |
| 17 | 300 | 85 | 15 | 23.5450 | 20.745 | 2.800 | 0.112 | 4.042 |
| 18 | 100 | 20 | 12 | 23.5282 | 22.4282 | 1.100 | 0.044 | 4.160 |
| 19 | 500 | 20 | 12 | 21.7516 | 18.6516 | 3.100 | 0.124 | 3.434 |
| 20 | 100 | 150 | 12 | 24.6315 | 24.4412 | 0.190 | 0.008 | 3.539 |
| 21 | 500 | 150 | 12 | 24.0811 | 21.9061 | 2.175 | 0.087 | 3.570 |
| 22 | 100 | 20 | 18 | 24.0850 | 22.035 | 2.050 | 0.082 | 3.700 |
| 23 | 500 | 20 | 18 | 22.3271 | 15.4521 | 6.875 | 0.275 | 3.765 |
| 24 | 100 | 150 | 18 | 24.8475 | 24.666 | 0.182 | 0.007 | 3.945 |
| 25 | 500 | 150 | 18 | 24.7528 | 20.1988 | 4.554 | 0.182 | 4.490 |
| 26 | 100 | 85 | 15 | 24.9209 | 23.7879 | 1.133 | 0.045 | 3.298 |
| 27 | 500 | 85 | 15 | 24.8132 | 19.9852 | 4.828 | 0.193 | 3.276 |
| 28 | 300 | 20 | 15 | 24.7834 | 21.0584 | 3.725 | 0.149 | 4.030 |
| 29 | 300 | 150 | 15 | 24.6866 | 22.9897 | 1.697 | 0.068 | 4.364 |
| 30 | 300 | 85 | 12 | 24.7711 | 22.1763 | 2.595 | 0.104 | 4.220 |
| 31 | 300 | 85 | 18 | 24.8224 | 20.2414 | 4.581 | 0.183 | 4.799 |
| 32 | 300 | 85 | 15 | 24.7496 | 21.1395 | 3.610 | 0.144 | 4.042 |
| 33 | 300 | 85 | 15 | 24.7039 | 21.1186 | 3.585 | 0.143 | 4.185 |
| 34 | 300 | 85 | 15 | 24.6779 | 20.984 | 3.694 | 0.148 | 4.089 |
| 35 | 100 | 20 | 12 | 24.7139 | 23.4877 | 1.226 | 0.049 | 3.685 |
| 36 | 500 | 20 | 12 | 24.7184 | 21.2446 | 3.474 | 0.139 | 2.980 |
| 37 | 100 | 150 | 12 | 24.9228 | 24.8363 | 0.087 | 0.003 | 3.395 |
| 38 | 500 | 150 | 12 | 24.8797 | 22.2609 | 2.619 | 0.105 | 3.593 |
| 39 | 100 | 20 | 18 | 24.7984 | 22.4785 | 2.3199 | 0.093 | 3.920 |
| 40 | 500 | 20 | 18 | 24.7319 | 17.9006 | 6.831 | 0.273 | 3.585 |
| 41 | 100 | 150 | 18 | 24.8542 | 24.6639 | 0.190 | 0.008 | 3.550 |
| 42 | 500 | 150 | 18 | 23.7129 | 19.1335 | 4.579 | 0.183 | 4.255 |
| 43 | 100 | 85 | 15 | 23.8594 | 22.6509 | 1.209 | 0.048 | 3.479 |
| 44 | 500 | 85 | 15 | 25.0749 | 20.1777 | 4.8972 | 0.196 | 3.327 |
| 45 | 300 | 20 | 15 | 24.1751 | 20.6251 | 3.550 | 0.142 | 4.380 |
| 46 | 300 | 150 | 15 | 24.1919 | 22.458 | 1.734 | 0.069 | 4.090 |
| 47 | 300 | 85 | 12 | 23.7506 | 21.156 | 2.595 | 0.104 | 4.270 |
| 48 | 300 | 85 | 18 | 23.7780 | 19.2056 | 4.572 | 0.183 | 4.365 |
| 49 | 300 | 85 | 15 | 24.8536 | 21.3273 | 3.526 | 0.141 | 4.145 |
| 50 | 300 | 85 | 15 | 24.2827 | 20.7868 | 3.496 | 0.140 | 4.180 |
| 51 | 300 | 85 | 15 | 23.4476 | 19.8683 | 3.579 | 0.143 | 3.835 |

**Table 3** Normalized data matrix

| Exp. no. | Normalized data matrix | |
|---|---|---|
| | MRR | $R_a$ |
| 1 | 0.005 | 0.528 |
| 2 | 0.025 | 0.362 |
| 3 | 0.000 | 0.396 |
| 4 | 0.012 | 0.464 |
| 5 | 0.011 | 0.483 |
| 6 | 0.084 | 0.415 |
| 7 | 0.001 | 0.557 |
| 8 | 0.039 | 0.691 |
| 9 | 0.002 | 0.435 |
| 10 | 0.035 | 0.390 |
| 11 | 0.015 | 0.654 |
| 12 | 0.006 | 0.634 |
| 13 | 0.010 | 0.618 |
| 14 | 0.031 | 0.802 |
| 15 | 0.013 | 0.627 |
| 16 | 0.014 | 0.590 |
| 17 | 0.013 | 0.587 |
| 18 | 0.002 | 0.622 |
| 19 | 0.016 | 0.424 |
| 20 | 0.000 | 0.450 |
| 21 | 0.008 | 0.458 |
| 22 | 0.007 | 0.492 |
| 23 | 0.078 | 0.509 |
| 24 | 0.000 | 0.559 |
| 25 | 0.034 | 0.724 |
| 26 | 0.002 | 0.391 |
| 27 | 0.038 | 0.386 |
| 28 | 0.023 | 0.583 |
| 29 | 0.005 | 0.684 |
| 30 | 0.011 | 0.640 |
| 31 | 0.035 | 0.827 |
| 32 | 0.021 | 0.587 |
| 33 | 0.021 | 0.629 |
| 34 | 0.023 | 0.601 |
| 35 | 0.002 | 0.488 |
| 36 | 0.020 | 0.319 |
| 37 | 0.000 | 0.414 |
| 38 | 0.011 | 0.464 |
| 39 | 0.009 | 0.552 |
| 40 | 0.077 | 0.462 |
| 41 | 0.000 | 0.453 |
| 42 | 0.035 | 0.650 |
| 43 | 0.002 | 0.435 |
| 44 | 0.040 | 0.398 |
| 45 | 0.021 | 0.689 |
| 46 | 0.005 | 0.601 |
| 47 | 0.011 | 0.655 |
| 48 | 0.034 | 0.684 |
| 49 | 0.021 | 0.617 |
| 50 | 0.020 | 0.628 |
| 51 | 0.021 | 0.528 |

**Table 4** Eigenvalues and proportions of principal components

| Principal component | Eigenvalues | Proportion (%) |
|---|---|---|
| First | 1.1357 | 56.8 |
| Second | 0.8643 | 43.2 |

**Table 5** Eigenvectors for principal components and contribution

| Quality characteristics | Eigenvectors | | |
|---|---|---|---|
| | First principal component | Second principal component | Contribution ($\beta_j$) |
| MRR | 0.707 | −0.707 | 0.376 |
| Surface roughness ($R_a$) | 0.707 | 0.707 | 0.256 |

where $a_{ij}$ is the performance quantity of the $i$th alternative on $j$th response, $n$ the number of attributes and $m$ the number of alternatives.

*Step 3:* Normalize the performance measure

The decision matrix is then normalized so that all the elements are dimensionless. This helps to compare the elements. Whether a response is beneficial or non-beneficial does not effect in normalization of the decision matrix. Normalization is generally carried out based on Eq. (2).

$$a_{ij}^* = \frac{a_{ij}}{\sqrt{\sum_{i=1}^{m} a_{ij}^2}} \quad (j = 1, 2, \dots, n) \tag{2}$$

where $a_{ij}^*$: Normalized value $i$th alternative on $j$th criteria$(0 < a_{ij}^* < 1)$.

*Step 4:* Assessment of overall assessment value

In the next step, these normalized performance measures are either added for beneficial criteria ("larger is better") or subtracted for non-beneficial ("lower is better") criteria. Based on previous literature [12, 32–34], overall assessment of the performance measure is defined by the following equation:

$$y_i = \sum_{j=1}^{g} a_{ij}^* - \sum_{j=g+1}^{n} a_{ij}^* \tag{3}$$

where $y_i$ is the normalized assessment value of $i$th alternative with respect to all the attributes, $g$ is the number of attributes to be maximized and $(n-g)$ is the number of attributes to be minimized.

It is true that, in a system, all the responses don't have a similar effect, and some are more dominant than others. Thus, to give added significance to any response, it could be multiplied with its respective weight (coefficient of

**Fig. 2** Overall assessment value graph

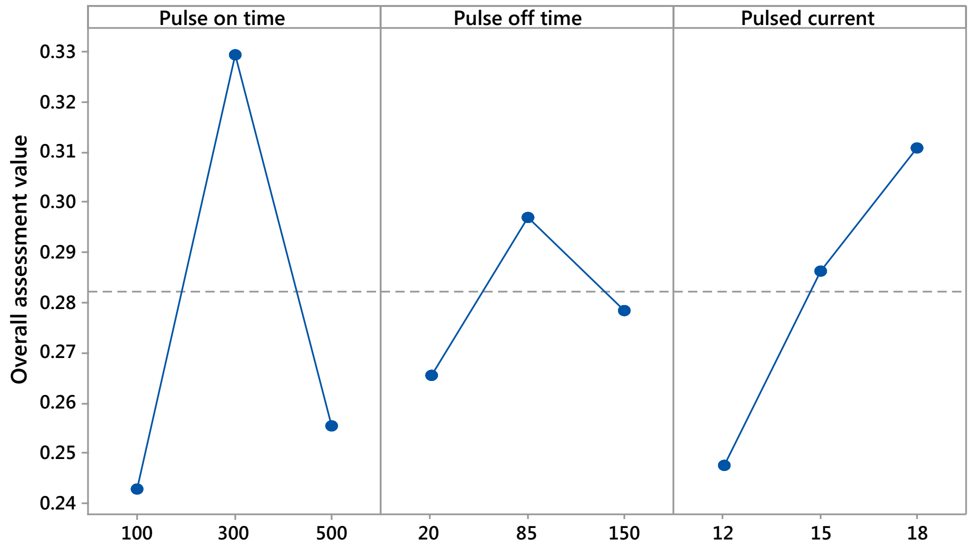


significance) [12, 32–35]. In this regard, the overall assessment value turns out to be:

$$y_i = \sum_{j=1}^{g} w_j a_{ij}^* - \sum_{j=g+1}^{n} w_j a_{ij}^* \tag{4}$$

where $w_j$ is the weight of $j$th criteria.

*Step 5:* Allocate ranking to the overall assessment

In the last step, the overall assessment values are sorted in descending order where the highest value of $y_i$ signifies the best alternate while the lowest value of $y_i$ signifies the worst.

### 2.6.2 Principal component analysis (PCA)

In 1901, Pearson [36] presented a statistical analysis method PCA. It initiates with a multi-response array with "$n$" experiments and "$m$" attributes. Subsequently, the following expression is used to get the correlation coefficient:

$$R_{jl} = \frac{\mathrm{cov}\left(x_i(j), x_i(l)\right)}{\sigma x_i(j) * \sigma x_i(l)} \tag{5}$$

where $x_i$ $(j)$ is the normalized values of each response. $\sigma x_i$ $(j)$ and $\sigma x_i$ (l): standard deviation of response variables $j$ and $l$. cov($x_i$ $(j)$, $x_i$ $(l)$): covariance of response variables $j$ and $l$.

Subsequently, eigenvalues and corresponding eigenvectors become:

$$\left(R - \lambda_x I_m\right) V_{ik} = 0 \tag{6}$$

where $\lambda_x$ are the eigenvalues.

$$\sum_{k=1}^{n} \lambda_k = n.$$

$$k = 1, 2, \ldots, n.$$

$V_{ik}\left[a_{k1,}a_{k2.......,}a_{km}\right]^{\mathrm{T}}$ are the eigenvectors corresponding to eigenvalue $\lambda_k$.

Thus, the principal components are:

$$Y_{mk} = \sum_{i=1}^{n} x_m(i) V_{ik} \tag{7}$$

where $Y_{m1}$ is the first principal component, $Y_{m2}$ the second principal component, and so on.

The principal components are ranked with respect to variance in descending order.

## 3 Results and discussion

In this study, to ascertain optimum machining condition for die-sinking EDM of Inconel 800, a hybrid MCDM approach MOORA-PCA is applied. Control variables and the corresponding responses of the experiment are shown in Table 2.

### 3.1 MOORA-PCA: hybrid approach

The alternatives studied in this research are $T_{\mathrm{ON}}$, $T_{\mathrm{OFF}}$ and $I_{\mathrm{p}}$, and attributes are MRR and surface roughness. The main aim was to minimize the surface roughness and to maximize the MRR which is a non-beneficial criterion. In Table 2, besides the experiment numbers, the last two columns (MRR and surface roughness) represent the decision matrix for the first step of the MOORA-PCA method. Their values are normalized to transform the several dimensional attributes into non-dimensional attributes. For all quality characteristics, the normalized values in each experimental run are determined using Eq. (2) (see Table 3).

**Table 6** Overall assessment value

| Exp. No. | $y_i$ | Rank |
|---|---|---|
| 1 | 0.266 | 31 |
| 2 | 0.193 | 50 |
| 3 | 0.198 | 48 |
| 4 | 0.238 | 36 |
| 5 | 0.247 | 34 |
| 6 | 0.249 | 32 |
| 7 | 0.279 | 28 |
| 8 | 0.365 | 4 |
| 9 | 0.218 | 44 |
| 10 | 0.212 | 45 |
| 11 | 0.335 | 9 |
| 12 | 0.320 | 15 |
| 13 | 0.314 | 17 |
| 14 | 0.417 | 2 |
| 15 | 0.320 | 14 |
| 16 | 0.302 | 23 |
| 17 | 0.300 | 24 |
| 18 | 0.312 | 18 |
| 19 | 0.220 | 41 |
| 20 | 0.225 | 40 |
| 21 | 0.233 | 38 |
| 22 | 0.249 | 33 |
| 23 | 0.294 | 25 |
| 24 | 0.279 | 27 |
| 25 | 0.379 | 3 |
| 26 | 0.196 | 49 |
| 27 | 0.212 | 46 |
| 28 | 0.303 | 21 |
| 29 | 0.344 | 7 |
| 30 | 0.325 | 11 |
| 31 | 0.431 | 1 |
| 32 | 0.304 | 20 |
| 33 | 0.325 | 12 |
| 34 | 0.311 | 19 |
| 35 | 0.245 | 35 |
| 36 | 0.169 | 51 |
| 37 | 0.207 | 47 |
| 38 | 0.237 | 37 |
| 39 | 0.280 | 26 |
| 40 | 0.269 | 30 |
| 41 | 0.226 | 39 |
| 42 | 0.342 | 8 |
| 43 | 0.219 | 42 |
| 44 | 0.219 | 43 |
| 45 | 0.355 | 6 |
| 46 | 0.303 | 22 |
| 47 | 0.333 | 10 |
| 48 | 0.359 | 5 |
| 49 | 0.319 | 16 |
| 50 | 0.324 | 13 |
| 51 | 0.275 | 29 |

Further, the relative weights of individual performance characteristics were estimated, using the PCA method, according to Eq. (6). The eigenvalues and proportions of principal components are shown in Table 4. The square value of the eigenvalues indicates the influence of the associated quality characteristics. Following PCA, the weightage for MRR and average Ra are determined as 0.4998 and 0.4998, respectively, which shows that within the studied input parameters range both the attributes are equally significant. Least surface roughness value contributes in getting a superior quality product, whereas high MRR contributes in accomplishing higher productivity. PCA model supports the same.

Using Eq. (4), the overall assessment value $y_i$ has been calculated (see Table 5). Ranking has been allotted to individual parameter setting according to hybrid MOORA-PCA method. After placing them in descending order, experiment no. 31 has the highest $y_i$ value. From Fig. 2, the higher the overall assessment value, the better multiple quality characteristics were. Therefore, the optimum combination of process parameters corresponds to $T_{\mathrm{ON}}2T_{\mathrm{OFF}}2I_{\mathrm{p}}3$, namely pulse-on time ($T_{\mathrm{ON}}$): 300 µs (level 2), pulse-off time ($T_{\mathrm{OFF}}$): 85 µs (level 2), and pulsed current ($I_{\mathrm{p}}$): 18 A (level 3), respectively, which yield the desired result (Table 6).

The response surface methodology (RSM) was executed to establish a mathematical relationship among the several EDM parameters and outputs. To study the effects of the several parameters on overall assessment value, a quadratic model (second-order polynomial equation) for the response surface was established. Using MINITAB 17, the model coefficients were assessed according to the least square method. The projected quadratic model to foresee the hybrid MOORA-PCA over the experimental region can be expressed using Eqs. (8) and (9).

$$\begin{aligned}\text{Overall assessment value} = {} & 1.308 \\ & + 0.000949T_{\mathrm{ON}} - 0.001881T_{\mathrm{OFF}} \\ & - 0.1525I_{\mathrm{p}} - 0.000003T_{\mathrm{ON}} * T_{\mathrm{ON}} \\ & + 0.000002T_{\mathrm{OFF}} * T_{\mathrm{OFF}} + 0.004876I_{\mathrm{p}} * I_{\mathrm{p}} \\ & + 0.000002T_{\mathrm{ON}} * T_{\mathrm{OFF}} + 0.000035T_{\mathrm{ON}} * I_{\mathrm{p}} \\ & + 0.000075T_{\mathrm{OFF}} * I_{\mathrm{p}}\end{aligned} \tag{8}$$

The quadratic model for the traditional MOORA can be expressed in Eq. (9).

$$\begin{aligned}\text{Overall assessment value} = {} & 2.623 \\ & + 0.001897T_{\mathrm{ON}} - 0.003762T_{\mathrm{OFF}} \\ & - 0.3059I_{\mathrm{p}} - 0.000005T_{\mathrm{ON}} * T_{\mathrm{ON}} \\ & + 0.000003T_{\mathrm{OFF}} * T_{\mathrm{OFF}} + 0.00978I_{\mathrm{p}} * I_{\mathrm{p}} \\ & + 0.000004T_{\mathrm{ON}} * T_{\mathrm{OFF}} + 0.000069T_{\mathrm{ON}} * I_{\mathrm{p}} \\ & + 0.000149T_{\mathrm{OFF}} * I_{\mathrm{p}}\end{aligned} \tag{9}$$

**Table 7** Error calculation for MOORA versus MOORA-PCA

| Exp. No. | MOORA | | | MOORA-PCA | | |
|---|---|---|---|---|---|---|
| | Experimental | Predicted | % error | Experimental | Predicted | % error |
| 1 | 0.533 | 0.551 | 3.315 | 0.266 | 0.275 | 3.439 |
| 2 | 0.387 | 0.397 | 2.584 | 0.193 | 0.197 | 2.062 |
| 3 | 0.396 | 0.420 | 6.061 | 0.198 | 0.210 | 6.017 |
| 4 | 0.476 | 0.524 | 10.084 | 0.238 | 0.229 | 3.678 |
| 5 | 0.494 | 0.534 | 8.097 | 0.247 | 0.268 | 8.359 |
| 6 | 0.499 | 0.546 | 9.439 | 0.249 | 0.273 | 9.63 |
| 7 | 0.557 | 0.522 | 6.367 | 0.279 | 0.271 | 2.867 |
| 8 | 0.730 | 0.752 | 3.014 | 0.365 | 0.363 | 0.435 |
| 9 | 0.437 | 0.414 | 5.263 | 0.218 | 0.202 | 7.318 |
| 10 | 0.425 | 0.429 | 0.91 | 0.212 | 0.214 | 1.123 |
| 11 | 0.669 | 0.632 | 5.561 | 0.335 | 0.316 | 5.697 |
| 12 | 0.640 | 0.657 | 2.656 | 0.320 | 0.329 | 2.661 |
| 13 | 0.629 | 0.654 | 4.038 | 0.314 | 0.327 | 4.155 |
| 14 | 0.833 | 0.781 | 6.235 | 0.417 | 0.390 | 6.384 |
| 15 | 0.640 | 0.730 | 14.063 | 0.320 | 0.315 | 1.617 |
| 16 | 0.604 | 0.630 | 4.253 | 0.302 | 0.315 | 4.247 |
| 17 | 0.600 | 0.630 | 4.948 | 0.300 | 0.315 | 4.942 |
| 18 | 0.624 | 0.551 | 11.752 | 0.312 | 0.304 | 2.564 |
| 19 | 0.439 | 0.394 | 10.19 | 0.220 | 0.197 | 10.464 |
| 20 | 0.450 | 0.420 | 6.659 | 0.225 | 0.210 | 6.705 |
| 21 | 0.466 | 0.487 | 4.506 | 0.233 | 0.229 | 1.611 |
| 22 | 0.499 | 0.536 | 7.381 | 0.249 | 0.268 | 7.489 |
| 23 | 0.587 | 0.546 | 6.968 | 0.294 | 0.273 | 7.15 |
| 24 | 0.559 | 0.522 | 6.702 | 0.279 | 0.261 | 6.602 |
| 25 | 0.758 | 0.727 | 4.072 | 0.379 | 0.363 | 4.113 |
| 26 | 0.393 | 0.404 | 2.867 | 0.196 | 0.202 | 3.085 |
| 27 | 0.424 | 0.429 | 1.148 | 0.212 | 0.214 | 1.123 |
| 28 | 0.606 | 0.632 | 4.257 | 0.303 | 0.316 | 4.262 |
| 29 | 0.689 | 0.657 | 4.645 | 0.344 | 0.329 | 4.502 |
| 30 | 0.651 | 0.654 | 0.522 | 0.325 | 0.327 | 0.63 |
| 31 | 0.862 | 0.781 | 9.389 | 0.431 | 0.390 | 9.425 |
| 32 | 0.608 | 0.630 | 3.567 | 0.304 | 0.315 | 3.561 |
| 33 | 0.650 | 0.630 | 3.125 | 0.325 | 0.315 | 3.13 |
| 34 | 0.623 | 0.630 | 1.074 | 0.311 | 0.315 | 1.23 |
| 35 | 0.490 | 0.551 | 12.381 | 0.245 | 0.255 | 4.082 |
| 36 | 0.339 | 0.394 | 16.303 | 0.169 | 0.192 | 13.609 |
| 37 | 0.414 | 0.420 | 1.457 | 0.207 | 0.210 | 1.407 |
| 38 | 0.475 | 0.459 | 3.375 | 0.237 | 0.229 | 3.271 |
| 39 | 0.561 | 0.536 | 4.486 | 0.280 | 0.268 | 4.412 |
| 40 | 0.539 | 0.465 | 13.729 | 0.269 | 0.273 | 1.48 |
| 41 | 0.453 | 0.522 | 15.129 | 0.226 | 0.234 | 3.54 |
| 42 | 0.685 | 0.727 | 6.151 | 0.342 | 0.363 | 6.261 |
| 43 | 0.437 | 0.404 | 7.491 | 0.219 | 0.202 | 7.741 |
| 44 | 0.437 | 0.429 | 1.861 | 0.219 | 0.214 | 2.109 |
| 45 | 0.710 | 0.632 | 11.014 | 0.355 | 0.335 | 5.634 |
| 46 | 0.606 | 0.657 | 8.416 | 0.303 | 0.329 | 8.42 |
| 47 | 0.666 | 0.651 | 2.252 | 0.333 | 0.327 | 1.788 |
| 48 | 0.719 | 0.781 | 8.632 | 0.359 | 0.390 | 8.741 |
| 49 | 0.638 | 0.738 | 15.674 | 0.319 | 0.315 | 1.308 |

**Table 7** (continued)

| Exp. No. | MOORA | | | MOORA-PCA | | |
|---|---|---|---|---|---|---|
| | Experimental | Predicted | % error | Experimental | Predicted | % error |
| 50 | 0.648 | 0.722 | 11.42 | 0.324 | 0.316 | 2.469 |
| 51 | 0.549 | 0.640 | 16.576 | 0.275 | 0.285 | 3.636 |
| Average error | | | 6.707 | 4.552 | | |

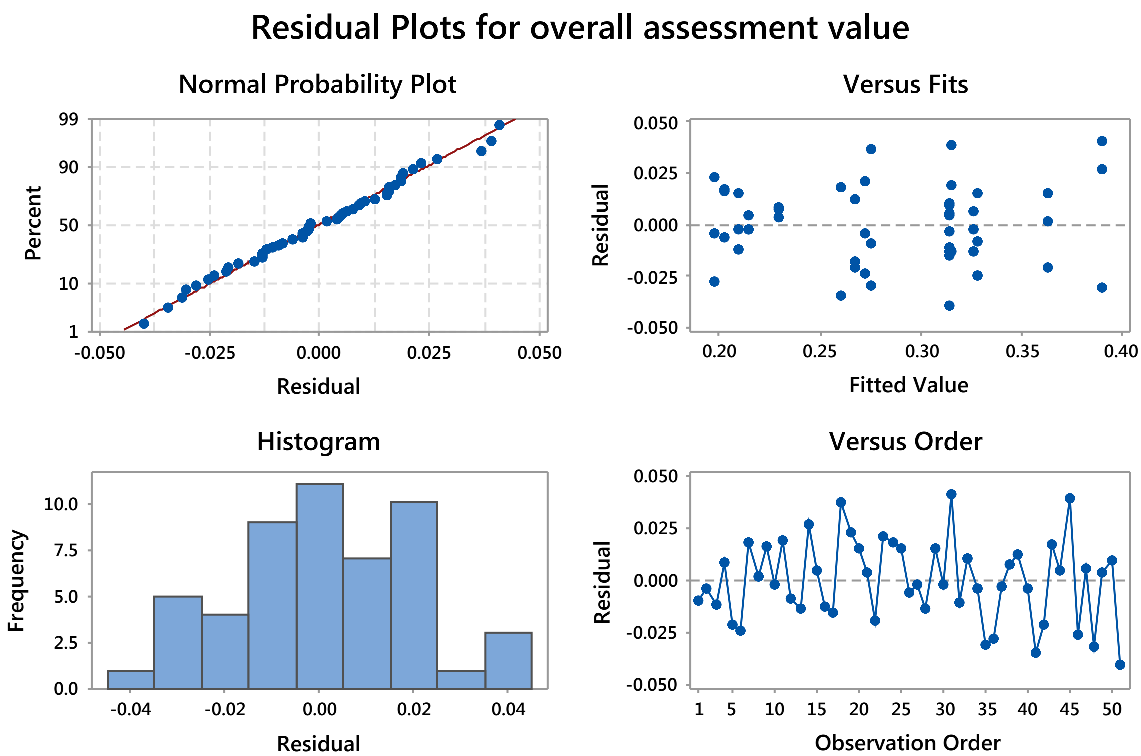


**Fig. 3** Residual plot for the overall assessment value for suggested MOORA-PCA method

To evaluate the accuracy of the prediction model, percentage error and average percentage error are calculated for both the conventional MOORA and advanced MOORA-PCA method (Table 7). For traditional MOORA, the maximum prediction error is 16.576%, but for advanced MOORA-PCA, the same is 13.609%. The average percentage error for conventional MOORA is 6.707, but for advanced MOORA-PCA the same is 4.552%. Subsequently, the prediction accuracy of the advanced MOORA model appeared more acceptable compared to the conventional MOORA.

To interpret the competence of the projected multivariate approach, a residual analysis was also carried out to check the model adequacy. It is one of the most important diagnostic tools to analyse model adequacy [37]. A normal probability plot of the standardized residual, standardized residual versus observation order and fitted value and the histogram is shown in Fig. 3, where there is no outlier and also the process follows a normal distribution. In normal probability plot, the residual points are following a straight line pattern which specifies the fitness of the suggested model. From Fig. 3, it is evident that standardized residuals and observation orders do not track any pattern or structureless. Hereafter, it might be recognized that the recommended model performs satisfactorily [19].

## 4 Conclusions

This paper highlights the application of multi-objective optimization technique MOORA coupled with PCA to recognize the optimal setting of the EDM parameters for machining Inconel 800. The experimental results and conclusions based are as follows:

- Comparison between hybrid MOORA-PCA and traditional MOORA shows the advantage of MOORA-PCA over MOORA method in optimizing the output responses in the present experimental environment
- A weight percentage of all attributes has been proposed to diminish the fluctuation nature of multi-objective optimization techniques model.
- According to MOORA-PCA approach, optimum setting of EDM parameters for the multi-objective quality characteristics was selected as $T_{on}2T_{off}2I_p3$, namely pulse-on time ($T_{ON}$): 300 µs, pulse-off time ($T_{OFF}$) 85 µs, and pulsed current ($I_p$): 18 A, respectively.

As a future scope, this method can be applied in the real-time manufacturing environment for a wider range of selection problems. However, the effect of various input parameters such as electrode shape and polarity on the performance characteristics was not investigated. These effects can be analysed in future works. FESEM analysis of machined surface is another important area in which further work can be followed up. The outcome of the present research work will be a considerable aid to the industries for quality improvement in processing using EDM for machining Inconel 800.

## References


1. Muthuramalingam T, Mohan B (2015) A review on influence of electrical process parameters in EDM process. Arch Civ Mech Eng 15(1):87–94
2. Tsai H, Yan B, Huang F (2003) EDM performance of Cr/Cu-based composite electrodes. Int J Mach Tools Manuf 43(3):245–252
3. Pachaury Y, Tandon P (2017) An overview of electric discharge machining of ceramics and ceramic based composites. J Manuf Process 25:369–390
4. Sharma P, Chakradhar D, Narendranath S (2017) Analysis and optimization of WEDM performance characteristics of Inconel 706 for aerospace application. Silicon 10(3):921–930
5. Majumder H, Maity K (2017) Optimization of machining condition in WEDM for titanium grade 6 using MOORA coupled with PCA—a multivariate hybrid approach. J Adv Manuf Syst 16(02):81–99
6. Ho K, Newman S (2003) State of the art electrical discharge machining (EDM). Int J Mach Tools Manuf 43(13):1287–1300
7. Khan A, Maity K (2016) Parametric optimization of some non-conventional machining processes using MOORA method. Int J Eng Res Afr 20:19–40
8. Chakravorty R, Gauri SK, Chakraborty S (2012) Optimization of correlated responses of EDM process. Mater Manuf Processes 27(3):337–347
9. Bhaumik M, Maity KP (2016) Multi response optimization by using the hybrid technique in electro discharge machining of AISI 304. Int J Eng Res Afr 26:68–75
10. Gadakh V (2011) Application of MOORA method for parametric optimization of milling process. Int J Appl Eng Res 1(4):743
11. Majumder H, Saha A (2018) Application of MCDM based hybrid optimization tool during turning of ASTM A588. Decis Sci Lett 7(2):143–156
12. Gadakh V, Shinde VB, Khemnar N (2013) Optimization of welding process parameters using MOORA method. Int J Adv Manuf Technol 69(9–12):2031–2039
13. Saha A, Mondal SC (2017) Multi-objective optimization of manual metal arc welding process parameters for nano-structured hardfacing material using hybrid approach. Measurement 102:80–89
14. Saha A, Mondal SC (2017) Multi-objective optimization of welding parameters in MMAW for nano-structured hardfacing material using GRA coupled with PCA. Trans Indian Inst Met 70(6):1491–1502
15. Adalarasan R, Santhanakumar M, Sundaram AS (2014) Optimization of weld characteristics of friction welded AA 6061–AA 6351 joints using grey-principal component analysis (G-PCA). J Mech Sci Technol 28(1):301–307
16. Adalarasan R, Sundaram AS (2015) Parameter design in friction welding of Al/SiC/Al2O3 composite using grey theory based principal component analysis (GT-PCA). J Braz Soc Mech Sci Eng 37(5):1515–1528
17. Paiva AP, Ferreira JR, Balestrassi PP (2007) A multivariate hybrid approach applied to AISI 52100 hardened steel turning optimization. J Mater Process Technol 189(1):26–35
18. Yih-Fong T, Fu-Chen C (2006) Multiobjective process optimisation for turning of tool steels. Int J Mach Mach Mater 1(1):76–93
19. Saha A, Mondal SC (2016) Multi-objective optimization in WEDM process of nanostructured hardfacing materials through hybrid techniques. Measurement 94:46–59
20. Rao TB, Krishna AG (2013) Simultaneous optimization of multiple performance characteristics in WEDM for machining ZC63/SiCp MMC. Adv Manuf 1(3):265–275
21. Saha A, Mondal SC (2018) Multi-criteria selection of optimal welding parameter in MMAW hardfacing using MOORA method coupled with PCA. Int J Mater Prod Technol 57(1–3):240–255
22. Saha A, Mondal SC (2019) Statistical analysis and optimization of process parameters in wire cut machining of welded nano-structured hardfacing material. Silicon 11:1313–1326. https://doi.org/10.1007/s12633-018-9924-y
23. Saha A, Mondal SC (2017) Machining optimization of nano-structured hardfaced tool insert in WEDM using MOORA method. In: International conference on research into design. Springer, Berlin
24. Saha A, Mondal SC (2017) Welding parameters optimization in MMAW assisted nano-structured hardfacing using desirability function analysis embedded with Taguchi method. In: International conference on research into design. Springer, Berlin
25. Ubaid AM et al (2017) Optimization of EDM process parameters with fuzzy logic for Stainless Steel 304 (ASTM A240)
26. Chandramouli S, Eswaraiah K (2017) Optimization of EDM process parameters in machining of 17-4 PH steel using Taguchi method. Mater Today Proc 4(2):2040–2047
27. Tomadi S et al (2009) Analysis of the influence of EDM parameters on surface quality, material removal rate and electrode wear of tungsten carbide. In: Proceedings of the international multiconference of engineers and computer scientists
28. Shashikant AKR, Kumar K (2014) Optimization of machine process parameters on material removal rate in EDM for EN19 material using RSM. IOSR J Mech Civ Eng 2320:24–28
29. Nikalje A, Kumar A, Srinadh KS (2013) Influence of parameters and optimization of EDM performance measures on MDN 300 steel using Taguchi method. Int J Adv Manuf Technol 69(1–4):41–49
30. Brauers WK (2004) Optimization methods for, vol 342. Kluwer Academic Publishers, Boston

31. Brauers WK, Zavadskas EK (2009) Robustness of the multi-objective MOORA method with a test for the facilities sector. Technol Econ Dev Econ 15(2):352–375
32. Karande P, Chakraborty S (2012) Application of multi-objective optimization on the basis of ratio analysis (MOORA) method for materials selection. Mater Des 37:317–324
33. Stanujkic D et al (2012) An objective multi-criteria approach to optimization using MOORA method and interval grey numbers. Technol Econ Dev Econ 18(2):331–363
34. Tansel İç Y, Yıldırım S (2013) MOORA-based Taguchi optimisation for improving product or process quality. Int J Prod Res 51(11):3321–3341
35. Siahaan APU, Rahim R, Mesran M (2017) Student admission assessment using multi-objective optimization on the basis of ratio analysis
36. Pearson K (1901) LIII. On lines and planes of closest fit to systems of points in space. Lond Edinb Dublin Philos Mag J Sci 2(11):559–572
37. Majumder H et al (2017) Use of PCA-grey analysis and RSM to model cutting time and surface finish of Inconel 800 during wire electro discharge cutting. Measurement 107:19–30